

Magneto-Roton Modes of the Ultra Quantum Crystal: Numerical Study

Pascal Lederer ^{+,◇,*} and ⁺C. M. Chaves

⁺*Departamento de Física, PUC-Rio, C. P. 38071, Rio de Janeiro and ^{+,◇}Instituto de Física, Universidade Federal do Rio de Janeiro, C.P.68528, 21945-970, Rio de Janeiro, Brasil*

(October 27, 2013)

The Field Induced Spin Density Wave phases observed in quasi-one-dimensional conductors of the Bechgaard salts family under magnetic field exhibit both Spin Density Wave order and a Quantized Hall Effect, which may exhibit sign reversals. The original nature of the condensed phases is evidenced by the collective mode spectrum. Besides the Goldstone modes, a quasi periodic structure of Magneto-Roton modes, predicted to exist for a monotonic sequence of Hall Quantum numbers, is confirmed, and a second mode is shown to exist within the single particle gap. We present numerical estimates of the Magneto-Roton mode energies in a generic case of the monotonic sequence. The mass anisotropy of the collective mode is calculated. We show how differently the MR spectrum evolves with magnetic field at low and high fields. The collective mode spectrum should have specific features, in the sign reversed "Ribault Phase", as compared to modes of the majority sign phases. We investigate numerically the collective mode in the Ribault Phase, and find in this latter case a previously unnoticed field independent low energy Magneto-Roton mode, at an intermediate wave vector. The occurrence of the Ribault Phase depends sensitively on the electron-electron interactions. A by product of our study deals with the metal-Ultra Quantum Crystal instability line: we find, in a monotonic sequence, a re-entrant behaviour of the metallic phase, at a given temperature, as a function of field, which has been observed experimentally. This behaviour also is sensitive to the strength of electron-electron interactions.

I. INTRODUCTION

When a static uniform magnetic field is applied perpendicular to their most conducting plane, certain Bechgaard salts undergo, at low temperatures, a transition from a metallic state to a cascade of Field Induced Spin Density Wave (FISDW) semi-conducting states; the latter exhibit a Quantized Hall Effect¹⁻⁵.

It is not fully recognized yet that this electron hole condensate is an original state of matter, which is neither a conventional Density Wave condensate nor a conventional Quantum Hall electronic liquid. The widely used phenomenological name of the phenomenon ("Field Induced Spin Density Waves") may be in part responsible for this oversight. This led one to propose the more correct name of "Ultra Quantum Crystal" (hereafter UQC)⁶. Indeed, in that system long range magnetic order (quantum crystal) sets in only because the unpaired carriers may form a few Landau bands (ultra quantum limit), while those Landau bands may organize and stay completely filled as the field varies only because magnetic order sets in. The Integer Quantum Hall Effect observed in the Bechgaard salts arises *because of* electron-electron interactions, in a three-dimensional material. This is in sharp contrast with the Integer Quantum Hall Effect in the two-dimensional electron gas⁷.

A clear sign of the unconventional nature of the electron-hole condensate in the UQC is that its condensation energy per particle is much smaller than the orbital energy. This precludes a perturbation treatment of the orbital magnetism in the theoretical description of the condensed phase.

Collective modes of the UQC are the clearest evidence for the specificity of the electron-hole condensate^{6,8,9}. Their spectrum exhibits an original structure in reciprocal space, with a series of local minima at multiples of G , the magnetic wavevector, which recall the local minimum of the Magneto-Roton (hereafter MR) mode at the inverse magnetic length in the Fractional Quantum Hall Effect⁷. The MR modes result both from the orbital motion of electrons, and from the condensation of a Density Wave order parameter. One might naïvely think of them as some sort of Kohn anomaly. However, Kohn anomalies, in quasi 1D conductors, are phonon local minima in the normal phase, at the wave vector $2k_F$. They become soft at the metal-CDW transition. The Magneto-Roton modes of the UQC never become soft. They appear at quantized values of the wave vector parallel component $q_{||} = G, 2G$, or, as we shall see for the UQC phases called Ribault Phases, and which are characterized by a negative Quantum Hall

*On leave from Physique des Solides, U. P. S., F91405 Orsay, France(Laboratoire associé au CNRS)

number, at nG , with $n = 4$ to 11. G is from three to two orders of magnitude smaller than k_F , depending on the magnetic field intensity: it does not relate to the Fermi Surface, but to the Quantum Hall Effect. It is equal to the change of wave vector from sub-phase to sub-phase and not to the subphase Density Wave wavevector.

It is a historical fact that, probably because of the advent of high temperature superconductivity, the experimental and theoretical effort about the UQC has slowed down considerably since 1986. In particular no experimental study has been published to test the theory of MR modes in the UQC, most of which dates back to 1987. Practically no theoretical progress either has been recorded since the first papers in 1987⁶ and 1988⁸.

Another plausible reason for the lack of experimental effort about the UQC collective modes is the lack of theoretical understanding, until recently, of the Quantum Hall sign inversion phenomenon, the so called Ribault anomaly. The latter was discovered early on¹⁰⁻¹², and was thought by some to be incompatible with the theory of the "usual" monotonic Quantum Hall Effect and UQC cascade phase diagram.

As will be discussed further on, the Ribault anomaly is now believed to be understandable within the same theoretical scheme, the "Quantum Nesting Model"(QNM), that allows to understand a good deal of the UQC phenomenology¹³. As a result, the other theoretical predictions of the QNM should be taken seriously and allowed to be tested experimentally in a detailed fashion.

This paper aims at bridging a gap between the theoretical state of affairs on the UQC collective modes, and the need for detailed quantitative predictions which could, and should, be compared to experiments. For instance, estimates of MR energies relative to the single particle gap, predictions about evolution of collective mode energies with magnetic field, estimates of MR effective mass anisotropy, were non existent until now.

We consider also phases with *negative* quantum Hall numbers, called "Ribault Phases", which have a qualitatively different spectrum from sub-phases with *positive* (majority sign) QHE⁹. In the negative sign QHE phase, MR have different (larger) *wave vectors*, different (larger) *energies*, and different *field dependences* when compared to the MR modes of the majority sign phases. Phases neighbouring the Ribault Phases, either in parameter space or in energy were predicted to have MR spectra intermediate between those of the normal phases and those of Ribault Phases.

For the first time detailed numerical estimates of the MR modes (within the Random Phase Approximation (RPA)) in the Ribault Phases, and the neighbouring phases are given, based on model parameter values which describe well the Bechgaard salts. In addition, with the particular set of parameters studied here, a new feature, previously unnoticed, emerges: a third MR mode, with lower energy (in most parts of the phase diagram) and almost no field dependence is predicted and computed. Furthermore, this study also reveals a large sensitivity of the sign reversal phenomenon to the strength of electron-electron interactions.

In order to compute the collective mode energies of the ordered phases, a first step deals with the computation of the metal-UQC instability line. This has yielded an interesting by-product: we have found that the QNM describes, on some occasions, a reentrance of the metallic phase at fixed temperature, as a function of magnetic field H , which is a well established experimental fact¹⁴. This reentrance was thought until now to be out of reach of the QNM.

Our paper is organised as follows: section II summarizes known results on the physics of Bechgaard salts under magnetic field. In section III we describe the results about the metal-UQC instability line; we emphasize the sensitivity of the phase diagram to the electron-electron interaction strength, in particular as regards the sign inversion phenomenon. We also discuss the re-entrant behaviour mentioned above. A summary of FISDW collective mode theory is given in section IV. New results on collective modes are described in section V which is divided in two parts: one describes the MR spectrum for the usual monotonic sequence of Quantum Hall phases, and shows how, as the field intensity is stepped up, UQC phases lose their field independent MR modes, and go over at high fields to a low energy excitation spectrum similar to that of a perfectly nested Spin Density Wave. The second part of section V gives the corresponding results for "Ribault Phases" (phases with Quantum Hall Effect sign inversion). We show there that the spectrum of MR modes exhibits qualitatively different features as compared to the monotonic sequence case. The same subsection also discusses the features of the MR spectrum in phases neighbouring the Ribault Phase in parameter space. A summary of the results and a discussion of their meaning is given in the Conclusion.

II. SUMMARY OF ULTRA QUANTUM CRYSTAL PHYSICS

Here we recall in more details some aspects of the physics of Bechgaard salts, and of their behaviour under magnetic field.

Organic conductors of the Bechgaard salts family, $(TMTSF)_2X$ where $TMTSF$ = tetramethylselenafulvalene are quasi-one-dimensional (quasi-1D) systems. The typical hierarchy of their transfer integrals is: $t_a = 3000K$, $t_b = 300K$, $t_c = 10K$. In three members of this family ($X = ClO_4, PF_6, ReO_4$), the metallic phase is destroyed by a moderate magnetic field H applied along the c direction, perpendicular to the most conducting planes (a, b). A cascade of magnetic phases, separated by first order transitions appears as the field intensity is stepped up: within each sub-

phase, a FISDW is stabilized with a peculiar electronic structure, characterized by a small number of exactly filled Landau levels (bands in fact)⁴. The Landau bands are separated by a hierarchy of gaps δ_n which oscillate with the magnetic field. The phase labelled by N is characterized by the largest gap δ_N at the Fermi level. A sum rule $\sum_n \delta_n^2 = \Delta^2$, connects all the gaps to the order parameter Δ .

Each UQC sub-phase exhibits a Quantized Hall conductivity, which is the first example of a Quantum Hall Effect in a 3D system. The cascade of quantized phases results from an interplay between the nesting properties of the Fermi Surface (FS), and the quantization of electronic orbits in the field: the wave vector of the SDW varies with field so that unpaired carriers in a subphase are always organized in completed filled Landau bands. As a result the number of carriers in each subphase is quantized, and so is the Hall conductivity: $\sigma_{xy} = 2Ne^2/\hbar^{1,4}$.

The condensation of the UQC phases results from the peculiar electronic structure of open Fermi Surface metal under magnetic field: because of Lorentz force, the electronic motion becomes periodic and confined along the high conductivity direction of the chains (\mathbf{a} direction)².

The periodic orbital motion of the electrons in real space is characterized by a wave vector $G = eHb/\hbar$, b being the interchain distance. The orbital wavelength x_0 is such that the flux threading the space between two organic chains over a length x_0 is one flux quantum ϕ_0 . As a result, the static bare susceptibility of the normal phase, $\chi_0(\mathbf{Q})$ can be expressed as a sum over weighted strictly 1D bare susceptibilities which diverge at quantized values of the longitudinal component of the wave vector $Q_{n,\parallel} = 2k_F + nG^{3-5}$. The largest divergence signals the appearance of a SDW phase with quantized vector $Q_{N,\parallel} = 2k_F + NG$.

It is important to realize that the periodic electronic motion along the a direction is manifest in a particular choice of gauge, the Landau gauge, when $\mathbf{A}_1 = (0, Hx, 0)$. With this choice, under the Peierls-Onsager substitution, the transverse electronic dispersion relation (which is periodic in $k_y b$), $\epsilon_{\perp}(k_y b, k_z c)$, becomes $\epsilon_{\perp}(k_y b - eHbx/\hbar, k_z c) = \epsilon_{\perp}(k_y b - Gx, k_z c)$, i. e. a periodic one-electron potential along a . With a different choice of gauge, say $\mathbf{A}_2 = (-Hy, 0, 0)$, the single electron Schrödinger equation is completely different, and no periodic potential appears along a , although the electronic spectrum is unchanged. This gauge dependent formulation is familiar for problems of orbital magnetism. In any particular choice of gauge, the potential vector breaks translational symmetry in a particular way, and single electron wave functions are gauge dependent. Energy spectra and macroscopic response functions are gauge independent.

The Quantized Nesting Model (QNM)⁵ describes most of the features of the phase diagram in a magnetic field. It has been shown recently to explain the experimental observation of the Hall plateaux sign reversal when the field varies¹³. Most plateaux exhibit the same sign. (By convention we will refer to these plateaux as positive ones). The sign reversal has been discovered by Ribault in $(TMTSF)_2ClO_4$ under certain conditions of cooling rate¹⁰. Negative plateaux have been reproduced and also found in $(TMTSF)_2PF_6$ where their existence depends crucially on pressure^{11,12,15}. Recently, Balicas et al¹⁵ have shown that there exists a range of pressure for which, in the PF_6 salt, the sequence of observed plateaux when the field decreases can be identified with the quantum numbers $N = 1, 2, -2, 3, 4, 5, 6, 7$. A more ancient experiment has shown a sequence of phases $N = 1, 2, -2, 4, -4, 5, 6$ ¹². Hereafter, we will refer to the UQC Phase with negative Hall number as "Ribault Phases".

Zanchi and Montambaux¹³ have shown that the negative plateaux can be understood within the QNM assuming the dispersion relation in the normal phase to be:

$$\begin{aligned} \epsilon(\mathbf{k}) &= v_F(|k_x| - k_F) + \epsilon_{\perp}(\mathbf{k}_{\perp}), \\ \epsilon_{\perp}(\mathbf{k}_{\perp}) &= -2t_b \cos k_y b - 2t_c \cos k_z c - 2t'_b \cos 2k_y b \\ &\quad - 2t_3 \cos 3k_y b - 2t_4 \cos 4k_y b \end{aligned} \quad (2.1)$$

$\epsilon(k_{\perp})$ is a periodic function which describes a warped FS. With $t_3 = t_4 = 0$, Eq.(2.1) cannot lead to sign reversals, as $sign(N) = sign(Q_{\parallel} - 2k_F) = sign(t'_b)$ ¹³. Small values of $t_3 \simeq .2t'_b = 2K$, and $t_4 = .2K$, however, are sufficient to account for the experimental results of Balicas et al. (A slightly different explanation for the negative Hall Effect phases has been put forward recently, based on the consideration of Umklapp terms¹⁶ and a non-zero t_4 term. We will not consider the Umklapp terms in this work.)

In Eq.(2.1), the only parameters which are not determined yet by experiments are t_3 and t_4 . Those parameters certainly exist as a correction to the linearized form of the dispersion relation along a , and they have to be small compared to $t'_b \simeq 10K$.

The normal metal-FISDW instability line $T_{cN}(H)$ is given by:

$$\chi_0(\mathbf{Q}, T_{cN}, H) = \sum_n I_n^2(Q_{\perp}) \chi_0^{1D}(Q_{\parallel} - 2k_F - nG, T_{cN}) = 1/\lambda \quad (2.2)$$

λ is the electronic interaction constant. Eq.(2.2) exhibits the structure of χ_0 as the sum of one dimensional terms χ_0^{1D} shifted by the magnetic field wave vector $G = eHb/\hbar$. $\chi_0^{1D} \propto -\ln(\max\{v_F(2k_F - q), T\}/\epsilon_F)$. In Eq. (2.2), the coefficient I_n depends on the dispersion relation and H:

$$I_n(Q_\perp) = \langle \exp i [T_\perp(p + Q_\perp/2) + T_\perp(p - Q_\perp/2)] + np \rangle \quad (2.3)$$

where $T_\perp(p) = (1/\hbar\omega_c) \int_0^p \epsilon_\perp(p') dp'$ and $\langle \dots \rangle$ denotes the average over p .

III. THE METAL-UQC INSTABILITY LINE

A. The sequence of UQC phases

Eq.(2.2) allows to compute the metal-UQC instability line. We show here that it is not sufficient, to determine the sequence of UQC phases, to examine the maxima of $\chi_0(\mathbf{q})$ as a function of \mathbf{q} at different fixed temperatures. This remark is especially meaningful in the description of the sign inversion phenomenon: depending on the value of λ in (2.2) different sequences of UQC phases emerge.

Define T_∞ as the FISDW ordering temperature in infinite field. In the latter case $I_n^2 = \delta_{n,0}$ and $\chi(q_\parallel = 2k_F, q_\perp = \pi/b) \propto \ln 2\gamma E_0/\pi T$. From Eq.(2.2), we have $T_\infty = (2\gamma/\pi)E_0 \exp(-1/\lambda)$. (γ is Euler's constant and E_0 a high energy cut-off). T_∞ is equal to the ordering temperature for the perfectly nested Fermi Surface at any field (i. e. when $t'_b = 0$). For a given value of the cut-off parameter E_0 , changing λ is equivalent to changing T_∞ . It is clear from Eq.(2.2) that the instability line results from the largest solution T_{cN} at a given field, among all solutions obtained by varying \mathbf{q} . Now define a generalized instability temperature $T_{N\pm m}(\pm q_\perp)$ as a lower temperature solution, i. e. one that corresponds to a larger free energy than the physical one; it corresponds, at a given field, to a different wave vector from that of the actual instability; for any integer m such that $q_\parallel - 2k_F = (N + m)G$, a whole family of solutions is obtained by varying q_\perp :

$$\frac{T_{N\pm m}}{T_\infty} = \exp \left[\sum_{n \neq 0} \frac{I_{N\pm m+n}^2(Q_\perp^N \pm q_\perp)}{I_{N\pm m}^2(Q_\perp^N \pm q_\perp)} \ln \left(\frac{\pi T_\infty}{2\gamma |n| \omega_c} \right) \right] \quad (3.1)$$

In Eq.(3.1), we have used the sum rule: $\sum_n I_n^2 = 1$. Eq.(3.1) is valid for all $k_B T < \hbar\omega_c$. For $m = 0$ and $q_\perp = 0$, $T_{N\pm m} = T_{cN}$, the ordering temperature for the N th subphase. For $m \neq 0$, $T_{N\pm m}(q_\perp)$ generalizes the definition of the critical temperatures on either side of phase N in the (T, H) plane. $T_{N\pm m}(q_\perp)$ are at most equal to the virtual transition lines $T_{N\pm m}$ which can be drawn in the N th subphase part of the phase diagram⁶. In the (T, H) plane, there is an infinite number of continuous lines crossing the phase diagram. The upper limit of this family is the actual (continuous non analytic) transition line from the normal metal to the UQC; this line coincides piecewise with the transition lines labelled by the successive integers describing the Quantum Hall conductivity¹⁷.

It is clear from inspection of Eq.(3.1) that T_{cN} *does not scale with* T_∞ , since the ratio T_{cN}/T_∞ on the left hand side of Eq.(3.1) depends on T_∞ through the argument of the logarithms on the right hand side. The variation of the ratio T_{cN}/T_∞ with T_∞ is complicated, with no clear tendency emerging at first sight because the coefficients $I_{N\pm m}$ have an oscillating behaviour as a function of their arguments $t_i/\hbar\omega_c$. Numerical results exhibit a rather sensitive dependence of the Quantum Hall sequence and of its sign changes with T_∞ , which is one of the new results of this paper.

T_∞ is not a free parameter: in our case, we are interested in a metallic ground state in the absence of field, therefore it cannot exceed t'_b/k_B , where t'_b violates the perfect nesting condition. t'_b has to exceed the value of the zero field SDW ordering temperature of the perfect nesting case, which is precisely equal to T_∞ .

The results of the numerical analysis for the transition line for different values of T_∞ are shown on Fig.(1) and Fig.(2) for two different choices of the parameters t_3 and t_4 .

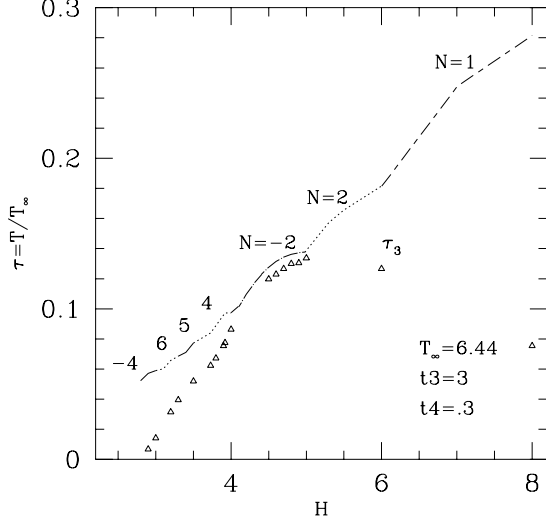


FIG. 1. Metal-FISDW instability line T_{cN} as a function of field for $T_{\infty} = 6.44\text{K}$. The values of the small parameters $t_3 = 3\text{K}$ and $t_4 = .3\text{K}$ are the same in Fig.(1) and Fig.(2). Notice the absence of phase $N = 3$.

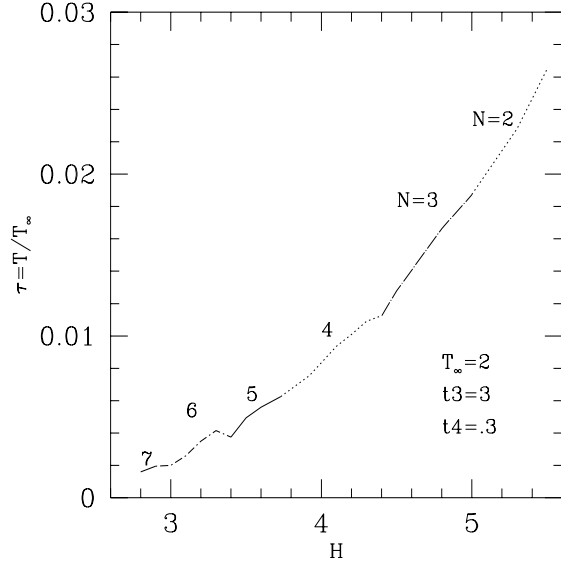


FIG. 2. Metal-FISDW instability line T_{cN} as a function of field for $T_{\infty} = 2\text{K}$. Substantial changes in the FISDW sequence of phases are observed in comparison with Fig.(1). The sequence of phases is monotonic (positive). The values of the small parameters $t_3 = 3\text{K}$ and $t_4 = .3\text{K}$ are the same in Fig.(1) and Fig.(2)

The dependence of the phase diagram is particularly clear when t_3, t_4 are both small compared to t'_b , as they should. In this latter case, the sign inversion phenomenon disappears altogether when T_{∞} is changed by a factor 3, from $T_{\infty} = 6.44\text{K}$ to $T_{\infty} = 2\text{K}$. The former value was used in previous work¹⁹ (see Fig.(1)). There is no sign inversion phenomenon when $T_{\infty} = 2\text{K}$, while the sequence of phases for $T_{\infty} = 6.44\text{K}$ is : $-4, 6, 5, 4, -2, 2, 1$. Note that phase -4 becomes stable, when the field increases, *before* phases 6 and 5, an unusual inversion of Hall number absolute

magnitude which has not yet been observed experimentally. Note also that the decrease of T_∞ by a factor 3 triggers a decrease of ordering temperatures by roughly two orders of magnitude between $H = 2.8$ T and $H = 5.3$ T.

For the choice of values $t_3 = 7$ K and $t_4 = .025$ K (taken from the literature¹³), the phase diagram also exhibits large changes upon a change of T_∞ from 6.44 K to 9 K. See Fig.(3) and Fig.(4). The sequence of phases 5, -4, 3, -2, 1 obtained at $T_\infty = 9$ K changes to the following: 5, -4, 4, 3, -2, 2, 1 when $T_\infty \rightarrow 6.44$ K: all other things equal, the change of T_∞ by less than 30% triggers the disappearance of phase 4, as well as changes of ordering temperatures by 600% to 200%.

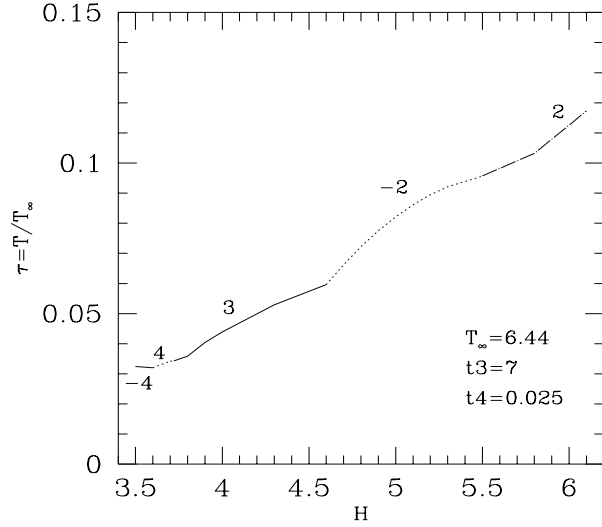


FIG. 3. Metal-FISDW instability line T_{cN} as a function of field for $T_\infty = 6.44$ K. Substantial changes in the FISDW sequence of phases are observed in comparison with Fig.(1). The values of the parameters $t_3 = 7$ K and $t_4 = .025$ K are the same in Fig.(3) and Fig.(4)

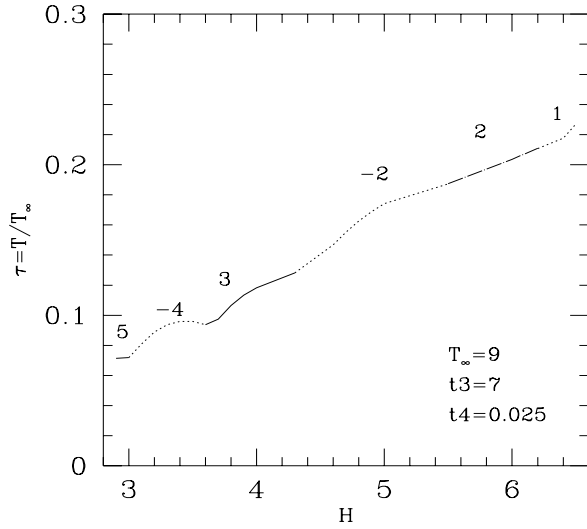


FIG. 4. Metal-FISDW instability line T_{cN} as a function of field for $T_\infty = 9$ K. In comparison with Fig.(2), phase $N = 4$ has vanished from the phase diagram. The values of the parameters $t_3 = 7$ K and $t_4 = .025$ K are the same in Fig.(3) and Fig.(4)

The sensitivity of the phase diagram, and especially of the magnitude of the ordering temperatures on T_∞ is such that knowing the phase Quantum Hall number and the value of the transition temperature at a given pressure allows a rather reliable experimental value for T_∞ .

B. Re-entrance of the metallic phase

Detailed experimental determination of the instability line has revealed that $dT_c(H)/dH$ may change sign as a function of H^{14} . This means that the metallic phase, at a fixed temperature exhibits a re-entrant behaviour as a function of field. This feature was thought to be outside the reach of the QNM in its usual formulation for the monotonic Quantum Hall number sequence because, until now the theoretical derivations of the transition lines within the QNM with $t_3 = t_4 = 0$ have not reproduced this feature. We have first found this behaviour in the numerical simulations with non zero values for t_3 and t_4 , as shown in Fig.(5). We have then studied this phenomenon as a function of t_3 and t_4 . The outcome of this study is that re-entrance appears already within the model with $t_3 = t_4 = 0$, within the framework of the monotonic sequence of Hall numbers, as shown on Fig.(5) and Fig.(6). It appears to depend also on the value of T_∞ .

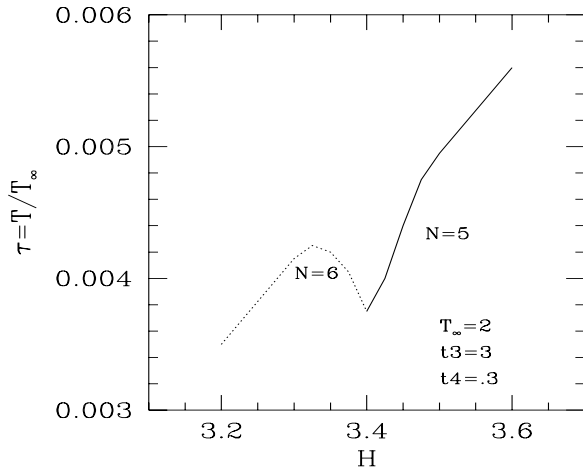


FIG. 5. Re-entrance of the Metal-FISDW instability line T_{cN} as a function of field for $T_\infty = 2\text{K}$. Here $t_3 = 3\text{K}$ and $t_4 = .3\text{K}$. However the re-entrant behaviour also exists within the model with zero value for both those parameters. See Fig.(6)

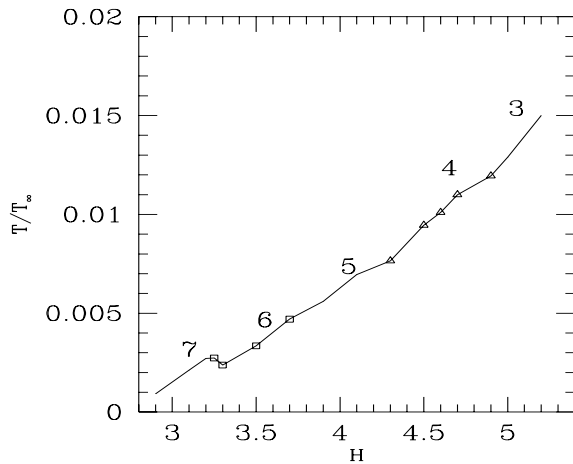


FIG. 6. Re-entrance of the Metal-FISDW instability line for $T_\infty = 2\text{K}$ and $t_3 = t_4 = 0\text{K}$

Our conclusion about this aspect of the phase diagram is that there is nothing mysterious about the re-entrant behaviour, which is well within reach of the simplest QNM; it is a simple consequence of the general shape of the $T_N(H)$ curves as function of field: each in turn goes through a maximum then decreases with field. If for a given N the maximum as a function of field is also the absolute maximum for all N values and for the same field, re-entrant behaviour follows.

IV. SUMMARY OF FISDW COLLECTIVE MODE THEORY

We now turn to the collective modes of the UQC which depend directly on the network of real and virtual transition lines defined in the last section. Using this network for the monotonic Quantum Hall sequence, ($t_3 = t_4 = 0$), Lederer and Poilblanc showed that the UQC collective modes exhibit, aside from the usual Goldstone modes linear in wave vector, at least one Magneto-Roton (hereafter MR) mode within the single particle gap, located at $q_{||} = G, 2G, \dots$, $q_z = \pi/c$, and some optimum q_y ^{6,8}. Only the mode at $q_{||} = G$ was actually proved to exist. Together with the usual Goldstone modes, it is the signature of the novel nature of the electron-hole condensate in UQC: a Spin Density Wave driven by orbital quantization and an Integer Quantum Hall system driven by electronic interactions. The MR mode is both a consequence of quasi 1D electronic periodic orbital motion, gauge invariance, and the long range crystalline order of the Field Induced Phase⁸.

The physical mechanism behind the MR minimum may be described as follows: the Goldstone boson at wave vector $q_{||} = mG$, in a usual SDW phase, is an overdamped mode, because $mv_F G = 2m\hbar\omega_c$, which is much larger than the single particle gap, at any value $m \geq 1$ ¹⁸. However, a fluctuation mode, in phase N , at a wave vector mG can scatter against the self consistent periodic orbital potential (responsible for the gaps at $\pm(k_F + mG)$ in the single particle dispersion relation) and shift its parallel momentum by $|mG|$, so as to propagate as a virtual mode with $q_{||} = 0$, i. e. a zero energy mode! However, it is not really a zero energy mode, as it would if the periodic orbital potential was a bona fide electrostatic potential, with bona-fide Bragg reflections. In fact this virtual shift in wave vector allows the mode at $q_{||} = mG$ to propagate in a medium which is not exactly like phase N for $q_{||} = 0$, but which is a mixture of unstable (excited) phases $N \pm m$. As we shall see, the closer the free energies of phases $N \pm m$ to that of phase N , the lower the MR energy within the single particle gap.

On the other hand, once the Quantum Hall sign inversion phenomenon is explained within the QNM, at the cost of refining the description of the electronic dispersion relation, the collective mode theory derived for the monotonic UQC sequence applies directly to the "Ribault Phase", the phase with inverted Quantum Hall sign⁹. This has a surprising consequence: exploiting the topology of the phase diagram in the presence of Hall Effect sign changes, one shows that the MR spectrum for the Ribault Phase -2 should be qualitatively different from the usual spectrum in the monotonic sequence case, so that the Ribault Phases are physically distinct from the majority sign UQC phases, and not just the same objects with negative carriers sign. For the particular sequence observed by Balicas et al.¹⁵, i.e. 1, 2, -2, 3, 4, 5, 6, 7, the differences in the -2 phase as opposed to the usual UQC subphase are the following:

- there are no MR modes with energy minimum at $q_{||} = G$ or at $q_{||} = 2G$
- there are at two MR modes with energy minimum at $q_{||} = 4G$ and $q_{||} = 5G$
- These MR modes have substantially higher energies than their usual counterparts. In particular, within the RPA, their energies are larger than half the single particle gap
- Both energy minima have a much larger field dependence than their normal counterparts
- those field dependences have opposite signs: the mode at $q_{||} = 4G$ is a decreasing function of the magnetic field, while the mode at $q_{||} = 5G$ is an increasing function of the magnetic field

Likewise, the MR spectrum of UQC phase N ($N > 0$) neighbouring the Ribault Phase $-|P|$ are "contaminated" by their neighbour, with one usual MR mode at $q_{||} = G$ and one mode at larger wave vector $q_{||} = mG = (|P| + N)G$, with large magnetic field dependence. This behaviour will be understood qualitatively from the equation for the mode energies in the following subsections; as for the modes within the Ribault phase, it is due to the dissymmetry between virtual phase energies for phases $N \pm m = N \pm (N + |P|)$ since $N + m$ and $N - m$ have opposite signs. Modes at G and $2G$ for $N > 1$ mix virtual phases $N \pm 1$ and $N \pm 2$ which both have free energies nearly equal to that of phase N . In contrast, for a phase with $N < 0$, the mode at mG mixes a low free energy virtual phase $N + m$ ($N + m > 0$) with a large free energy one $N - m$ ($N - m < 0$).

A. The dynamic spin-spin correlation function

Technically MR energies have been derived within the RPA^{6,8}, by looking at the poles of the spin-spin correlation function of the ordered phase.

This can be shown by explicit microscopic computation of the transverse dynamic spin-spin correlation function $\chi_{+-}(q, \omega)$ in the RPA, by extending the work of Lee Rice and Anderson on collective modes in CDW phases²⁰.

Letting

$$\tilde{\sigma}_+ = \psi_{2\uparrow}^+(\bar{x}) \psi_{1\downarrow}(\bar{x})$$

and

$$\tilde{\sigma}_- = \psi_{1\downarrow}^+(\bar{x}) \psi_{2\uparrow}(\bar{x})$$

where $\psi_{\alpha\sigma}^+(\bar{x})$ is the creation field operator for a particle of spin σ on sheet α of the Fermi surface, at space time coordinate $\bar{x} \equiv (\vec{r}, t)$; then we can define

$$\chi_{\alpha\beta} = -\langle T_\tau \tilde{\sigma}_\alpha(\bar{x}) \tilde{\sigma}_\beta(\bar{x}') \rangle \quad \alpha \neq \beta$$

$$\Gamma_{\alpha\alpha} = -\langle T_\tau \tilde{\sigma}_\alpha(\bar{x}) \tilde{\sigma}_\alpha(\bar{x}') \rangle e^{i\alpha \vec{Q}_N(\bar{x} + \bar{x}')}$$

The dynamic susceptibility in the ordered phase, as well as the off diagonal response function $\Gamma_{\alpha\alpha}$ can be obtained within the RPA, from the non interacting response function, defined as follows

$$\chi_{+-}^{0F}(\bar{x}, \bar{x}') = G_{22}(\bar{x}, \bar{x}') G_{11}(\bar{x}', \bar{x})$$

$$\Gamma_{++}^{0F}(\bar{x}, \bar{x}') = G_{21}(\bar{x}, \bar{x}') G_{21}(\bar{x}', \bar{x})$$

$G_{jj}(\bar{x}, \bar{x}')$ is the propagator for the field operator on side j of the Fermi surface. $G_{ij}(\bar{x}, \bar{x}')$ (with $i \neq j$) is the anomalous propagation in the presence of the non zero order parameter. Here 1 and 2 represent $1 \uparrow$ and $2 \downarrow$. The RPA yields the following expression

$$\begin{aligned} \chi_{+-}^F(\vec{Q} = \vec{Q}_N + \vec{q}, \omega) &= \\ \chi_{+-}^{0F}(\vec{Q}_N + \vec{q}, \omega) - \lambda \left[\chi_{+-}^{0F}(\vec{Q}_N + \vec{Q}, \omega) \chi_{+-}^{0F}(\vec{Q}_N, \vec{q}, \omega) - \Gamma_{--}^{0F}(\vec{q}, \omega) \Gamma_{++}^{0F}(\vec{q}, \omega) \right] & \\ \frac{\left[1 - \lambda \chi_{+-}^{0F}(\vec{Q}_N - \vec{q}, \omega) \right] \left[1 - \lambda \chi_{+-}^{0F}(\vec{Q}_N + \vec{q}, \omega) \right] - \lambda^2 \Gamma_{--}^{0F}(\vec{q}, \omega) \Gamma_{++}^{0F}(\vec{q}, \omega)}{\Gamma_{--}^F(\vec{q}, \omega)} &= \\ \frac{\Gamma_{--}^{0F}(\vec{q}, \omega)}{\left[1 - \lambda \chi_{+-}^{0F}(\vec{Q}_N - \vec{q}, \omega) \right] \left[1 - \lambda \chi_{+-}^{0F}(\vec{Q}_N + \vec{q}, \omega) \right] - \lambda^2 \Gamma_{--}^{0F}(\vec{q}, \omega) \Gamma_{++}^{0F}(\vec{q}, \omega)} & \end{aligned}$$

Those formulas are quite general. In the usual case of SDW in zero magnetic field, they simplify because of the symmetry $\vec{q} \rightarrow -\vec{q}$, i.e. $\chi_{+-}^{0F}(\vec{Q}_N - \vec{q}, \omega) = \chi_{+-}^{0F}(\vec{Q}_N + \vec{q}, \omega)$, so that

$$\chi_{+-}^F(\vec{Q}_N + \vec{q}, \omega) \pm \Gamma_{--}^F(\vec{q}, \omega) = \frac{\chi_{+-}^{0F}(\vec{Q}_N + \vec{q}, \omega) \pm \Gamma_{--}^{0F}(\vec{q}, \omega)}{1 - \lambda(\chi_{+-}^{0F}(\vec{Q}_N + \vec{q}, \omega) \pm \Gamma_{--}^{0F}(\vec{q}, \omega))}$$

The latter expression leads to the phase and amplitude modes of the SDW, once one uses the gap equation

$$\chi_{+-}^{0F}(\vec{Q}_N, \omega = 0) - \Gamma_{--}^{0F}(\vec{q} = 0, \omega = 0) = \frac{1}{\lambda}$$

The simplified expression is still approximately valid, in the limit $|\vec{q}| \ll \frac{2\pi}{x_0}$, for the Ultra Quantum crystal. For a general \vec{q} , however, the correct collective mode equation is given by the poles of $\chi_{+-}^F(\vec{Q}_N + \vec{q}, \omega) \pm \Gamma_{--}^F(\vec{q}, \omega)$, i.e. by the equation

$$\left[1 - \lambda \chi_{+-}^{0F}(\vec{Q}_N - \vec{q}, \omega) \right] \left[1 - \lambda \chi_{+-}^{0F}(\vec{Q}_N + \vec{q}, \omega) \right] = \lambda^2 \Gamma_{--}^{0F}(\vec{q}, \omega) \Gamma_{++}^{0F}(\vec{q}, \omega)$$

B. Collective mode equation

The electronic orbital motion, together with the RPA treatments of interactions, results in effective scattering potential energy terms which couple electron states with wave vector $k_{||}$ and $k_{||} + 2k_F + nG$, (n integer) on either side of the Fermi Surface. This results in a series of gaps in the condensed phase dispersion relation⁴, corresponding to the various potential scattering terms. The simplest approximation which captures the essential physics resums to all orders the gap $\delta_N = I_N \times \Delta$ at the Fermi level and takes all other gaps into account to second order in perturbation^{6,8}. The limit $2\delta_n/\omega_c \ll 1$ is assumed to hold. Then the equation for collective modes in the UQC phase N reduces to:

$$\left(\ln \left(\frac{2\gamma E_0}{\pi T_{N+m}} \right) - \tilde{\chi}_0(\delta, \omega) \right) \left(\ln \left(\frac{2\gamma E_0}{\pi T_{N-m}} \right) - \tilde{\chi}_0(\delta, \omega) \right) = \left(\tilde{\Gamma}_0(\delta, \omega) \right)^2 \quad (4.1)$$

where $T_{N\pm m}$ is defined in Eq.(3.1), and $q_{||} = 2k_F + (m + \delta)G$, with $\delta \ll 1$.

$\tilde{\chi}_0$ and $\tilde{\Gamma}_0$ are for $n = 0$ the objects discussed in²⁰ in connections with collective modes of SDW. Eq.(4.1) finally yields, setting $x_{N,m} = \omega(q_{||}/G = m + \delta, q_{\perp})/(2\delta_N)$, (with $q_z = \pi/c$):

$$\left(\ln \left(\frac{T_{cN}}{T_{N+m}} \right) - (x_{N,m}^2 - 1/2)h(x_{N,m}) \right) \left(\ln \left(\frac{T_{cN}}{T_{N-m}} \right) - (x_{N,m}^2 - 1/2)h(x_{N,m}) \right) = h^2(x_{N,m})/4 \quad (4.2)$$

with $h(x, T) = \int_0^{\infty} du \frac{\tanh(\frac{\delta_N}{2T} \cosh u)}{\cosh^2 u - x^2}$. In the limit $T = 0K$, $h(x, T \rightarrow 0)$ reduces to

$$h(x) = \frac{\sin^{-1} x}{x(1-x^2)^{1/2}}, \quad x < 1$$

C. Analytical results

Define $\epsilon_{\pm m} = (T_{cN} - T_{N\pm m})/T_{cN}$

Simple solutions are found for Eq.(4.2) in the limit that $\epsilon_{\pm m} \ll 1$. Then

$$x_{N,m}^2 \simeq (\epsilon_{-m} + \epsilon_{+m})/2$$

. Since ϵ_{-m} and ϵ_{+m} have roughly equal and opposite variations with magnetic field within phase N , the MR minimum is roughly field independent. In general, in most of the parameter space of a given phase, $\epsilon_{\pm m} > .3$ except for $m = 1$, so that accurate results demand a numerical solution. In particular a numerical analysis is required to determine whether a solution exists or not within the single particle gap for $m > 1$. In order to find the lowest energy solution, one must vary the momentum transverse component in Eq.(3.1). However, another simple solution holds in the case that $\epsilon_m \ll 1$, while $\epsilon_{-m} \simeq 1$. This situation, as we shall see, is of interest in the case of the Ribault Phase. It is then straightforward to show from Eq.(4.2) that $x_m^2 \simeq 1/2 + (6/\pi)\epsilon_m - \pi/(\ln(T_{cN}/T_{-m})) \simeq 1/2$. In most other cases, a numerical solution of Eq.(4.2) proves necessary.

The following section presents the results of our detailed numerical analysis.

V. THE SPECTRUM OF MR MODES

A. The monotonic Quantum Hall number sequence

We now exploit the results of the last section. First we derived, at $T = 0K$, the MR mode spectrum in a generic case: a phase well within a monotonic sequence of UQC phases. We picked phase $N = 4$. Then we study the differences which arise at high field, for the last two phases of the monotonic sequence: $N = 1$ and $N = 0$.

1. The generic case

The parameters we took for the numerical estimates are relevant to the Bechgaard salts, and have been used previously in the literature¹⁷: $t_a = 3000K$, $t_b = 265K$, $t'_b = 10K$, $T_{\infty} = 6.44$. (Those parameters may change with pressure, notably t'_b).

The results are shown on Fig.(7). We find two modes, at $q_{||} = G$ or $2G$ which vary little with H , and a *third mode*, rather close to the upper edge of the gap, at $q_{||} = 6G, q_{\perp} = 0$. This mode is yet another example of "contamination" by the Ribault phase $N = -2$ discussed in the next subsection⁹. It has a monotonic H negative variation, and drowns into the single particle continuum for $H \lesssim 3.75T$.

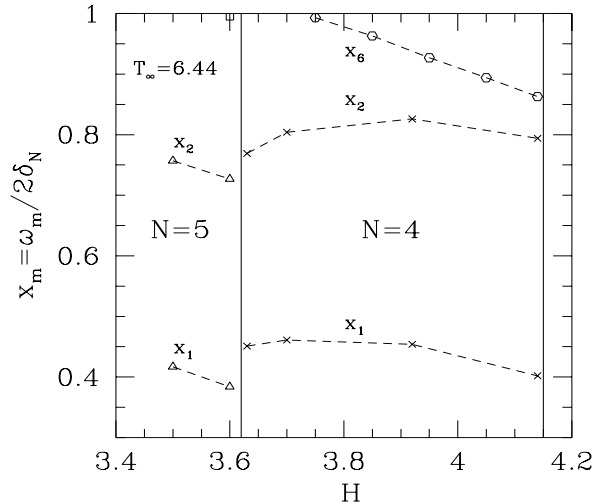


FIG. 7. Energy minima of the MR modes in phase $N = 4$ of the monotonic Quantum Hall sequence ($t_3 = t_4 = 0K$). The lowest energy mode has $q_{||} = G$, the intermediate energy MR mode has $q_{||} = 2G$, the highest energy mode is field dependent and has $q_{||} = 6G$ and couples to the virtual phase at $N = -2$. It is due to "contamination" of the Ribault phase at $N = -2$.

We have looked for MR mode with $q_{||} = 8G$, in phase 4, which might arise from contamination of the near-by Ribault phase $N = -4$, and found it did not exist in the absence of additional terms in Eq.(2.1), but this mode will certainly become alive under pressure^{13,9}.

The RPA evaluation yields a MR minimum $x_{5,1}^{min} \simeq .4$, located at $q_{\perp}^{min} = .0178/b$ for $H = 3.6T$. By varying q_{\perp} around q_{perp}^{min} at fixed q_{vert} , we can compute the transverse MR mode dispersion. We find a *very large* mass anisotropy $m_{\perp}/m_{||}|_{N=5,m=1} \simeq .9 \times 10^3$, with $m_{||} = \hbar\omega_{min}/v_F^2$. The fact that $x_{5,1} < 1/2$ makes this MR mode a good candidate for the kind of specific heat anomalies discussed in ref⁽⁴⁾. The mass anisotropy is larger for the mode $q_{||} = 2G$, we find $\simeq 2.25 \times 10^3$. See Fig.(8). The MR energy ω_{Nm}^{min} is discontinuous at the transition from N to $N \pm 1$. This contributes a (small) term, which corrects the mean field estimate to the transition latent heat. On the other hand, $\omega_{4,6}^{min}$ goes continuously at the transition to $N = 3$ into $\omega_{3,5}^{min}$ (i. e. a *distinct* MR with the *same* energy). The computed MR dispersion relation is shown on Fig.(8).

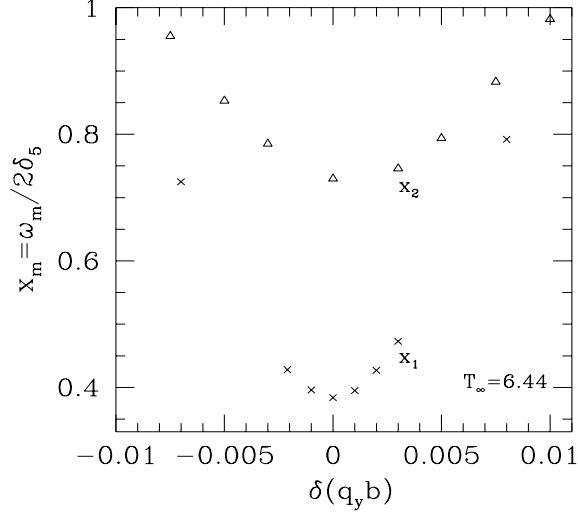


FIG. 8. Dispersion of the MR modes in the transverse direction for the two low energy modes in UQC phase 5; crosses correspond to the mode with $q_{\parallel} = G$; triangles correspond to the mode with $q_{\parallel} = 2G$; results are similar for phase 4. The effective mass m_{\perp} is found to be about 10^3 larger than m_{\parallel} .

2. Large magnetic fields

The situation changes for $H > 6.1$ T, the critical value for the transition from UQC phases 2 to 1. The reason for this change is apparent from the $T(H)$ curve in Fig.(10): in phase 1, the mode at $q_{\parallel} = G$ continues to mix two virtual phases with free energies close to the the free energy of phase 1, i.e. phases 0 and 2. But the mode at $q_{\parallel} = 2G$ mixes two virtual phases with widely different free energies: phase 0 (with free energy close to that of phase 1) and phase -1 which has a very low (virtual) ordering temperature T_{-1} . Similarly, in phase $N = 0$, both modes at $q_{\parallel} = G$ and $2G$ mix a low energy phase (resp. $N = 1$ and $N = 2$) with high energy ones (resp. $N = -1$ and $N = -2$). As the free energy difference between phase $N = 0$ and phase $N = 1, 2$ increases rapidly as the field increases, the MR mode energies at $q_{\parallel} = G$ and $2G$ increase rapidly with field. This is seen in Fig.(9).

The two MR modes which exist in the low field part of phase $N = 1$ have different field dependences. The high energy mode, with $q_{\parallel} = 2G$ increases its energy monotonically with field, at a rate $\simeq 1.2\delta_1/T$, then merges into the single particle continuum for $H \gtrsim 7$ T. Then only one MR at $q_{\parallel} = G$ survives, at lower energy, and with a non monotonic field dependence. In fact the rate of variation of $\omega_{1,1}^{min}/2\delta_1$ is also large, $\simeq -1.8/T$ for $H \gtrsim 7.5$ T. For $H \lesssim 6.5$ T, $d\omega_{1,1}^{min}/dH \simeq .8\delta_1/T$.

At the transition from $N = 1$ to $N = 0$, at $H \simeq 8.25$ T, two MR modes appear discontinuously. The MR at $q_{\parallel} = G$ is 21% higher in energy in phase 0, and that at $q_{\parallel} = 2G$ is close to the single particle continuum, at $.95 \times 2\delta_0$. In fact this latter mode is also connected to the "contamination" of the Ribault phase at $N = -2$, since it connects T_2 and T_{-2} as described by Eq.(3.1)⁹. Both MR energies increase rapidly with H , at a rate $\simeq \delta_0/T$ for the low energy mode, $1.6\delta_0/T$ for the high energy one.

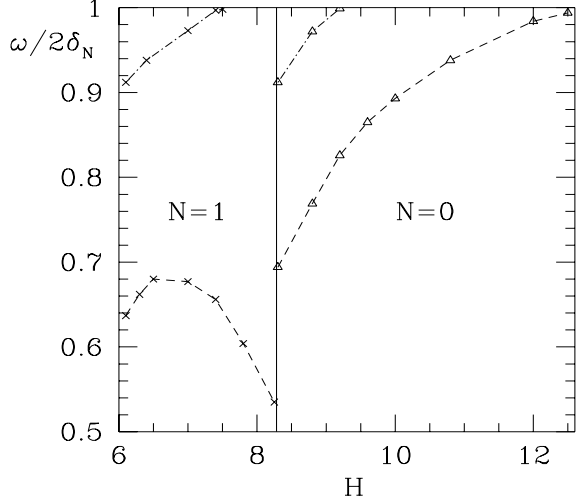


FIG. 9. Variation of the MR energy minima with magnetic field at large fields. The lowest MR mode at $q_{\parallel} = G$ in phase $N = 1$ has a qualitatively different behaviour as a function of field than the mode at $2G$ in phase $N = 1$ and those at G (low energy) and $2G$ (high energy) in phase $N = 0$. This behaviour stems from the network of real and virtual transition lines depicted in Fig.(10)

The last surviving MR dissolves into the single particle continuum for $H \gtrsim 12.5$ T. For larger H the only collective modes left are the usual Goldstone modes at $q_{\parallel} \ll G$. Then the only specific features of the UQC left are small single particle energy gaps, at most an order of magnitude smaller than the FS gap, at large energies $\hbar\omega_c$, $2\hbar\omega_c$, etc..

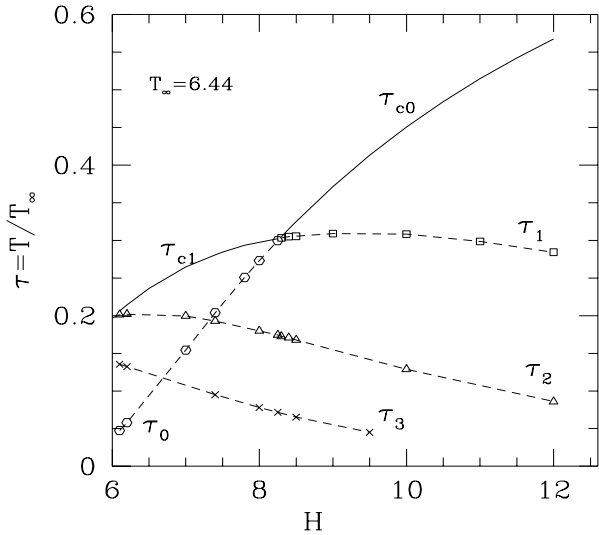


FIG. 10. Network of real and virtual transition lines of the UQC phase diagram at large fields. For $H > 8.1$ T, the free energy difference between the thermodynamically stable phase $N = 0$ and the unstable phases 1 and 2 increases rapidly with field.

The low energy physics of the $N = 0$ phase for $H \gtrsim 12.5$ T is thus identically that of an insulating SDW phase with perfect nesting FS.

The actual field values for which the MR mode drowns in the continuum in phase $N = 0$ cannot be taken too

seriously, since for that range of field values, the approximation $2\delta_0/\hbar\omega_c \ll 1$ breaks down completely. However, the behaviour found above holds qualitatively since the approximation becomes good again at higher fields.

In this section, besides proving that within the RPA, more than one MR mode is usually alive in the single particle gap, at $q_{||} = G$ or $2G$ (possibly $3G$, or $5, 6, 7, 8G$ etc. due to the vicinity of Ribault phases, as we shall see in the next section) and computing their energies as a function of field, we have derived for the first time numerical estimates of the very large effective mass anisotropy of the MR. We have described how, as the magnetic field increases, UQC phases at small quantum numbers progressively lose their MR and, above a threshold field, retrieve a low energy excitation spectrum of a conventional SDW with perfect nesting. In the following, we examine how the situation changes in the case of the Ribault Phase.

B. MR modes of the Ribault Phase and neighbouring phases

We now turn to the Quantum Hall sign inversion phenomenon. Specifically, we are interested in the following Quantum Hall number sequence: $\dots 6, 5, 4, -2, 2, 1$, which corresponds to the UQC cascade shown on Fig.(1) (Notice that no phase $N = 3$ is thermodynamically stable in Fig.(1)). Investigating the MR spectrum of phase $N = -2$, we now have, from Eq.(4.1), the following possibilities:

- Both $N + m$ and $N - m$ are ≤ 0 . Then $T_{N \pm m}$ are so small that no MR mode can exist within the single particle gap. This preclude MR modes to exist for $m = 1$ or $m = 2$.
- Or $(N + m)(N - m) < 0$. Then one of the virtual transition lines, say T_{-2+m} may be close to $T_{c-2}(H)$, but the other one is very close to zero. Then a MR mode may exist around $q_{||} = mG$, with relative energy $\omega_m/2\delta_2 \geq 1/\sqrt{2}$.

As a consequence, the MR spectrum in the Ribault Phase $N = -2$ exhibits the following qualitative features⁹: there are no modes at $q_{||} = G$, or $2G$ but two higher energy modes exist at $q_{||} = 4G$ and $q_{||} = 6G$; they have large magnetic field dependences of opposite sign; the two modes cross roughly in the center of phase -2 in the phase diagram. In addition, we find a third, almost field independent MR at $q_{||} = 5G$ which was not described in ref.⁽⁹⁾. In this latter work, Hall sign inversion was studied among a complete sequence of integers, as opposed to the sequence where one, or more than one, integer is missing, such as the sequence discussed here: $\dots 6, 5, 4, -2, 2, 1$. In the latter case the mode $q_{||} = 5G$ is due to the existence of a virtual phase at $N = 3 = -2 + 5$ the free energy of which is only slightly above that of phase -2 : the two corresponding lines are practically parallel within the whole $N = -2$ phase, while the "associate" phase at $N = -7 = -2 - 5$ has very large free energy. i. e. very small values of T_{-7} . This is another case of contamination from a nearly stable phase. As discussed above, the corresponding MR mode is then field independent, and its value relative to the single particle gap of phase -2 is close to $1/\sqrt{2}$. See Fig.(11).

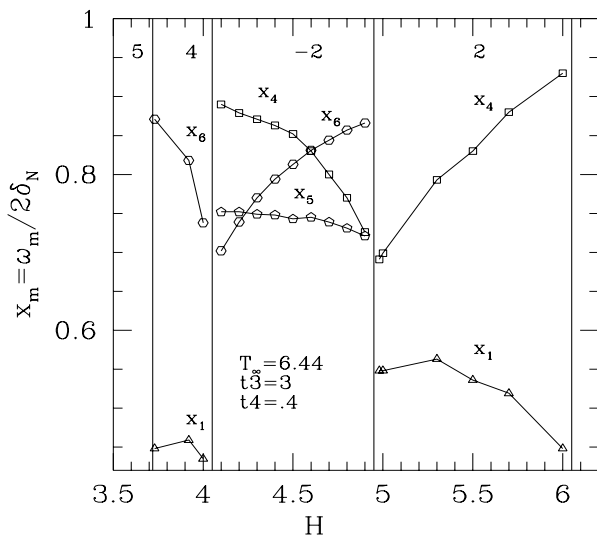


FIG. 11. Spectrum of MR energy minima in the Ribault phase $N = -2$ for the following Quantum Hall number sequence: 6,5,4,-2,2,1. Within phase $N = -2$, the MR modes at $4G$ ($6G$) mix a low free energy virtual phase $N = 2$ ($N=4$) with a high free energy one, $N = -6$ ($N=-8$). The almost field independent mode at $5G$ stems from the coupling to phase $N = 3$. The difference in free energy between phases $N = 3$ and $N = -2$ is almost constant.

Another feature apparent in Fig.(11) is the qualitatively different behaviour of modes at G and $4G$ (resp $6G$) as a function of magnetic field in phase $N = 2$ (resp $N = 4$). The reason for this difference in behaviour is that the mode at G couples two virtual phases with low free energies (e.g. phases 1 and 3 for the mode at G in phase 2); the latter vary with opposite sign as a function of magnetic field. On the other hand the mode at $4G$ in phase 2 couples two phases with very different free energies: low energy phase -2 and high energy phase 6. Then according to Eq.(4.2), the low free energy virtual phase dictates its field dependence to the MR mode.

It is obvious that even richer MR spectra are expected when the FISDW phase diagram has more sign reversals. The closer those sign reversed phases in parameter space, the more complex the MR spectrum: this is because there are more virtual UQC phases with free energies close to that of the stable one. See for example the network of virtual transition lines within phase $N = -4$ in Fig.(12).

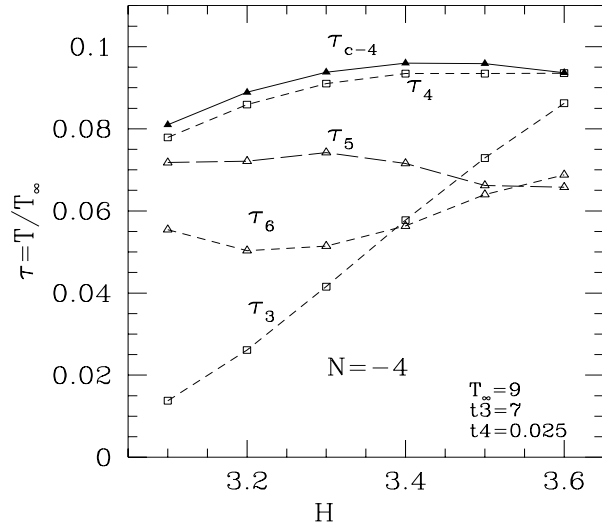


FIG. 12. Network of virtual transition lines within phase $N = -4$ for the Quantum Hall number sequence 6,5,-4,3,2,-2,1. The peculiar behaviour of MR mode 10 in Fig.(13) with field stems from the non monotonic variation of $T_6(H)$. MR mode 8 in Fig.(13), on the contrary is field independent because the two curves $T_{c,-4}$ and T_4 stay close to one another.

This network of virtual transition lines gives rise to the MR spectrum shown in Fig.(13).

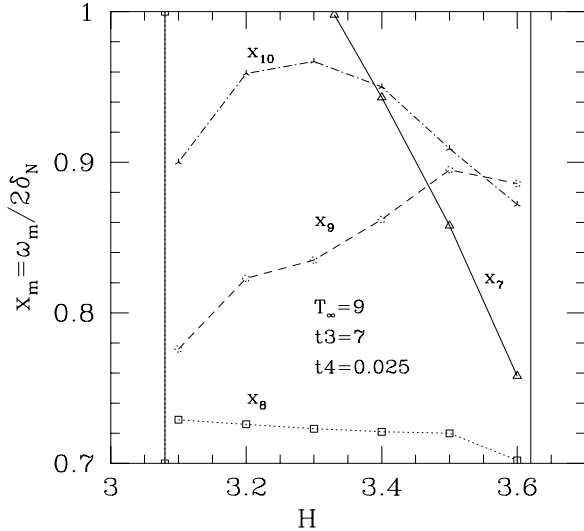


FIG. 13. Spectrum of MR energy minima in the Ribault Phase -4 for the Quantum Hall number sequence 6,5,-4,3,2,-2,1. The loci of MR minima are one order of magnitude further away from the origin than the lowest MR minimum at $q_{||} = G$ in the generic positive phase.

VI. CONCLUSION

In view of the renewed confidence in the Quantum Nesting Model as a valid description of the Field Induced Spin Density Wave phenomenon in Bechgaard salts, we have developed the theoretical consequences of the model as regards the collective modes of the UQC.

Our effort has developed in two main directions:

- We give detailed numerical predictions regarding the collective mode spectrum when the phase diagram has no FISDW with negative Quantum Hall number (monotonic Quantum Hall sequence). In that case we have proved numerically the existence, within the RPA, of a second MR mode with $q_{||} = 2G$ within the single particle energy gap, in the generic case. Both low energy modes at G and $2G$ are almost field independent in the whole domain of stability of a given phase. In addition, a strongly field dependent mode at larger parallel wave vector may propagate within the single particle gap because of "contamination" from a virtual phase with negative Quantum Hall number, when the latter is almost stable. The mass anisotropy of the MR modes are computed for the first time. The parallel to in-plane transverse mass ratio is of order 10^3 .

Then we have studied the MR spectrum of phases with quantum numbers 1 and 0, i.e. phases at large field (typically $H \gtrsim 6T$). We show that the two low energy modes become field dependent, their energies increase with field and, in the case of the $N = 0$ phase, they merge in the single particle excitation continuum. Above a threshold field which we have computed, the low energy physics of the FISDW is that of a perfectly nested SDW phase.

- We have turned to the case of the UQC phase cascade with Quantum Hall sign inversion. This unique phenomenon of the Quantum Hall Effect physics, observed only in the Bechgaard salts, leads to a different structure in the collective mode MR spectra of the sign reversed phases. There are no modes with $q_{||} = G$ or $2G$; there are modes centered at larger wave vectors, with larger energies, and with different field dependences; in the case of cascades with various sign reversals, there might be four, or more, modes in the single particle gap with wave vectors an order of magnitude larger than in the monotonic cascade case.

In the course of this latter study, which involves two poorly known small parameters t_3 and t_4 which correct the normal metal electronic dispersion relation, we have shown that the cascade phase diagram, besides depending sensitively on t_3 and t_4 ¹³ depends also sensitively on the electron-electron interaction parameter T_{∞} : a change of this parameter by a factor 3 may suppress altogether the sign inversion phenomenon. The metal/UQC instability line does not scale with T_{∞} .

We have also found that the model contains the (experimentally observed) possibility of metallic re-entrance at fixed temperature as a function of field; this may happen also when $t_3 = t_4 = 0$.

Our results are obtained within the RPA, in the "very weak" coupling limit ($2\delta_N/\hbar\omega_c \ll 1$). In Bechgaard salts, this ratio is of order .4 below 6 T, and increases with field. Between 8 T and 20 T, it is actually larger than 1, then it decreases and becomes small at very large fields. Thus, significant corrections may be expected, in a weak coupling RPA, (i. e. $\lambda \ll 1$) to all estimates derived here, in particular between 8 T and 20 T. We have found that the lowest MR energy minima of the positive UQC phases could be sometimes below δ_N . Those values might be significantly lowered by self-trapping effects, which are outside the scope of linear response theory. However the presence of MR with $x_{N,m} < .5$ does not seem to be guaranteed for all N . The effective masses should increase due to MR-MR scattering processes, etc.. The importance of those effects will be gauged by comparing experimental values to the estimates given here. The latter should be a useful guideline to determine the MR parameters.

We have provided a number of new quantitative and qualitative predictions on the spectrum of FISDW collective modes, derived from the QNM model which should help experimentalists in the detection of these original fluctuation modes of an original electron-hole condensate.

- ¹ For recent reviews, see L. P. Gor'kov, J.Phys. I France **6**, 1697 (1996); P. M. Chaikin, *ibid*, p. 1875; P. Lederer, *ibid*, p. 1899; V. M. Yakovenko and H.S. Goan, *ibid*, p. 1917
- ² L. P. Gor'kov and A. G. Lebed, J. Physique. Lett. **45**, L433, (1984); P. M. Chaikin, Phys. Rev. **B 31**, 4770 (1985)
- ³ G. Montambaux, Physica Scripta, **T 35**, 188 (1991).
- ⁴ P. Lederer, J. Phys. I France **6**, 1899 (1996)
- ⁵ M. Héritier, G. Montambaux and P. Lederer, J. Physique Lett. **45**, L943, (1984). See also K. Yamaji, J. Phys. Soc. Jap. **54**, 1034, (1985)
- ⁶ P. Lederer and D. Poilblanc, C. R. Acad. Sc. Paris, **304**, II-251 (1987).
- ⁷ The Quantum Hall Effect, Girvin and R. E. Prange and S. M. Girvin, ed. (Springer Verlag 1987), chap. IX.
- ⁸ D. Poilblanc and P. Lederer Phys. Rev. **B 37**, 9650 (1988); **B 37**, 9672 (1988)
- ⁹ P. Lederer preprint cond-mat 9707338
- ¹⁰ M. Ribault, Mol. Cryst. Liq. Cryst. **119**, 91 (1985).
- ¹¹ B. Piveteau *et al* J. Phys. C **19**, 4483 (1986)
- ¹² J. R. Cooper, *et al* Phys. Rev. Lett. **63**, 1984 (1989); S. T. Hannahs *et al*, Phys. Rev. Lett. **63**, 1988 (1989).
- ¹³ D. Zanchi and G. Montambaux, Phys. Rev. Lett. **77**, 366 (1966)
- ¹⁴ F. Tsobnang, F. Pesty and P. Garoche Phys. Rev. **B 49**, 15110, (1994)
- ¹⁵ L. Balicas, G. Kriza and F. I. B. Williams, Phys. Rev. Lett. **75**, 2000 (1995).
- ¹⁶ N. Dupuis and Victor M. Yakovenko, cond-mat 9712216
- ¹⁷ P. Lederer and G. Montambaux Phys. Rev. **B 37**, 5375 (1988)
- ¹⁸ It can be a real long lived excited mode in one of the energy gaps of the single particle dispersion relation, around $n\hbar\omega_c$, (n integer).
- ¹⁹ D. Poilblanc, Thèse, Orsay 1987.
- ²⁰ P. A. Lee, T. M. Rice and P. W. Anderson, Sol. St. Com. **14**, 703 (1986).
- ²¹ D. Poilblanc, G. Montambaux, M. Héritier, P. Lederer, Phys. Rev. Lett. **58**, 270, (1987).